ORIGINAL ARTICLE

Meshless upwind local radial basis function-finite difference technique to simulate the time- fractional distributed-order advection–diffusion equation

Mostafa Abbaszadeh[1] · **Mehdi Dehghan**[1]

Abstract

The main objective in this paper is to propose an efficient numerical formulation for solving the time-fractional distributed-order advection–diffusion equation. First, the distributed-order term has been approximated by the Gauss quadrature rule. In the next, a finite difference approach is applied to approximate the temporal variable with convergence order $\mathcal{O}(\tau^{2-\alpha})$ as $0 < \alpha < 1$. Finally, to discrete the spacial dimension, an upwind local radial basis function-finite difference idea has been employed. In the numerical investigation, the effect of the advection coefficient has been studied in terms of accuracy and stability of the proposed difference scheme. At the end, two examples are studied to approve the impact and ability of the numerical procedure.

Keywords Radial basis functions (RBFs) · Finite difference (FD) scheme · Fractional convection–diffusion · Time-fractional distributed-order advection–diffusion equation · Local meshless method · Upwind method

1 Introduction

The fractional PDEs with distributed-order derivative are solved by some approaches such as multi-fractal memory kernels [37], the matrix approach [35], a novel difference procedure [28], compact difference technique [43], two ADI difference schemes [25], second-order finite difference approximation [53], discontinuous spectral element methods [52], hybrid functions approximation [32], and discontinuous Galerkin method [41].

Recently, Atangana and Baleanu [6] developed a new fractional derivative to describe some questions in the field of fractional calculus. Authors of [7] convoluted Riemann–Liouville–Caputo derivative with the Mittag–Leffler function for the Atangana–Baleanu fractional differential operators. The model of transmission dynamics of vector-borne diseases is proposed in [3] to the concept of fractional differentiation and integration. Authors of [31] considered a new time distributed-order and two-sided space-fractional advection–dispersion equation.

The RBF-FD method has been introduced in [21, 23, 24]. Author of [38] developed a generalization of the RBF-FD method that computes RBF-FD weights in finite-sized neighborhoods around the centers of RBF-FD stencils. The local RBF method has been used for solving some models such as high-dimensional time-fractional convection–diffusion equation [36], the convection-dominated diffusion problems [39], and incompressible viscous Navier–Stokes equations [26].

The time-fractional distributed-order advection–diffusion equation is

✉ Mostafa Abbaszadeh
  m.abbaszadeh@aut.ac.ir

  Mehdi Dehghan
  mdehghan@aut.ac.ir; mdehghan.aut@gmail.com

1 Department of Applied Mathematics, Faculty
  of Mathematics and Computer Science, Amirkabir
  University of Technology, No. 424, Hafez Ave.,
  Tehran 15914, Iran

$$
\begin{cases}
\displaystyle\int_0^1 w(\alpha)\,{}_0^C D_t^\alpha u(\mathbf{x},t)\mathrm{d}\alpha = \Delta u(\mathbf{x},t) - v \cdot \nabla u(\mathbf{x},t) + f(\mathbf{x},t), & (x,y) = \mathbf{x} \in \Omega, \quad 0 < t \le T, \\[2mm]
u(\mathbf{x},0) = \psi(\mathbf{x}), & (x,y) = \mathbf{x} \in \Omega, \\[2mm]
u(\mathbf{x},t) = g(\mathbf{x},t), & (x,y) = \mathbf{x} \in \partial\Omega.
\end{cases}
\tag{1}
$$

Also, for $w : [0,1] \to \mathbb{R}$, we have the following conditions:

$$
\forall\, \alpha \in [0,1], \quad w(\alpha) > 0, \quad \text{and}
$$

$$
\int_0^1 w(\alpha)\mathrm{d}\alpha = W > 0.
$$

Furthermore, ${}_0^C D_t^\alpha$ denotes

$$
\begin{aligned}
\frac{\partial^\alpha u(x,y,t)}{\partial t^\alpha} &= {}_0^C D_t^\alpha u(x,y,t) \\
&= \frac{1}{\Gamma(1-\alpha)} \int_0^t \frac{\partial u(x,s)}{\partial s} \frac{\mathrm{d}s}{(t-s)^\alpha}, \quad \alpha \in (0,1).
\end{aligned}
\tag{2}
$$

The Legendre wavelet approach has been proposed in [44] for the solution of the linear and nonlinear distributed fractional differential equations. A novel second-order numerical approximation for the Riemann–Liouville tempered fractional derivative is derived in [17] using the tempered Grünwald difference operator and its asymptotic expansion. The numerical solution of distributed-order time-fractional PDEs is studied in [33] based on the mid-point quadrature rule and linear B-spline interpolation. The main aim of [29] is to discuss the properties of the time-tempered fractional derivative, and studying the well-posedness and the Jacobi-predictor–corrector algorithm for the tempered fractional ordinary differential equation. The Keller Box method is used in [34] to spatially discretise the fractional subdiffusion equation. Author of [18] developed fourth-order fractional-compact difference operator to solve the time–space tempered fractional diffusion-wave equation. A new high-order numerical algorithm and its error analysis are developed in [19] for solving the Riesz tempered space-fractional diffusion equation. Authors of [20] developed a class of high-order numerical algorithms for Riesz derivatives based on constructing new generating functions.

The aim of [4, 5] is to prove the existence of the solution to the Cauchy problem for the time distributed-order diffusion equation as well as to calculate it. Authors of [10] proposed diffusion-like equations with time- and space-fractional derivatives of the distributed order for the kinetic description of anomalous diffusion and relaxation phenomena. Authors

of [11] provided explicit strong solutions and stochastic analogs for distributed-order time-fractional diffusion equations on bounded domains with Dirichlet boundary conditions. The main aim of [30] is to study the uniqueness and existence solution of the boundary value problems for the generalized time-fractional diffusion equation of distributed order over an open bounded domain. Author of [45] developed efficient algorithms based on the Legendre-tau approximation for one- and two-dimensional fractional Rayleigh–Stokes problems for a generalized second-grade fluid.

The Jacobi–Gauss–Lobatto (J–G–L) collocation approach is used in [9] to solve the distributed-order time- and Riesz space-fractional Schrödinger equation (DOT–RSFSE). Authors of [47] constructed and analyzed a Legendre spectral-collocation method for the numerical solution of distributed-order fractional initial value problems. The main aim of [48] is applying a Legendre collocation method for solving distributed-order fractional optimal control problems. Two efficient spectral algorithms based on the Jacobi–Galerkin methods are proposed in [27] for solving unsteady advection–reaction–diffusion equations with constant and variable coefficients. Authors of [46] derived the generalized necessary conditions for optimal control problems with dynamics described by ordinary distributed-order fractional differential equations (DFDEs) and then they proposed an efficient numerical scheme for solving an unconstrained convex distributed optimal control problem governed by the DFDE. Existence and uniqueness of solutions of a nonlinear tempered fractional boundary value problems are studied in [49]. Author of [50] derived and analyzed an exponentially accurate Jacobi spectral-collocation method for the numerical solution of nonlinear terminal value problems involving the Caputo fractional derivative. Author of [50] proved that the convergence rate for non-smooth solutions can be enhanced using a suitable smoothing transformation, which allows us to adjust a parameter in the solution in view of a priori known regularity of the given data. A Legendre–Jacobi collocation approach is developed in [51] for solving a nonlinear system of two-point boundary value problems with derivative orders.

Author of [1] proposed an error estimate of second-order finite difference scheme for solving the Riesz space

distributed-order diffusion equation. The main aim of [13] is to propose a new numerical scheme based on the spectral element procedure for simulating the neutral delay distributed-order fractional damped diffusion-wave equation. The main aim of [2] is to combine the alternating direction implicit approach with the interpolating element-free Galerkin method to solve two-dimensional distributed-order time-fractional diffusion-wave equation. A finite element method has been proposed in [14] for solving the Rayleigh–Stokes problem for a heated generalized second-grade fluid with fractional derivatives. An error estimate has been proposed in [15] to solve the two-dimensional weakly singular integro-partial differential equation with space and time-fractional derivatives based on the finite element/finite difference scheme. Authors of [16] applied the homotopy analysis method to solve nonlinear fractional partial differential equations such as the fractional KdV, $K(2, 2)$, Burgers, BBM-Burgers, cubic Boussinesq, coupled KdV, and Boussinesq-like $B(m, n)$ equations.

In the advection–diffusion equation, there are two important constants, e.g., advection and diffusion parameters [12]. The main difficulty of this equation is when the advection constant is larger than the diffusion parameter in which there are a few numerical procedures that solve the mentioned problems to find an acceptable result. In the current paper, we employ an upwind local RBF-FD technique to overcome the mentioned difficulty. Also, we could solve this equation on the non-rectangular domains.

2 Semi-discrete scheme

To discrete the time variable and integral term, we employ the following notations:

$$t_k = k\tau, \quad \tau = \frac{T}{N}, \quad k = 0, 1, \dots, N,$$

$$h_\alpha = \frac{1}{2J}, \quad \alpha_l = 1 + lh_\alpha, \quad 0 \le l \le 2J.$$

At first, we want to discrete the integral term in the model (1)

Lemma 2.1 [8] *The Gaussian–Legendre integration is*

$$\int_{-1}^{1} f(x)\mathrm{d}x = \sum_{j=1}^{n} w_j f(x_j) + E_n(f), \quad \forall f(x) \in C^\infty[-1, 1],$$

(3)

where x_j are roots of Legendre polynomial $P_n(x)$ and weights are defined as

$$w_j = \frac{-2}{(n+1)P_n{}'(x_j)P_{n+1}(x_j)}, \quad j = 1, 2, \dots, n.$$

(4)

We employ the following notations:

$$u^{n-\frac{1}{2}} = \frac{1}{2}\left(u^n + u^{n-1}\right), \quad \delta_t u^{n-\frac{1}{2}} = \frac{1}{\tau}\left(u^n - u^{n-1}\right),$$

where $u^n = u(x, y, t_n)$.

Lemma 2.2 [40] *Suppose $0 < \alpha < 1$ and $g(t) \in C^2[0, t_k]$, it holds that*

$$\left| \frac{1}{\Gamma(1-\alpha)} \int_0^{t_k} \frac{v'(t)}{(t_k - t)^\alpha} \mathrm{d}t - {}^C\mathcal{P}_t^\alpha(v(t)) \right|$$

$$\le C_\alpha \max_{0 \le t \le t_k} |v''(t)| \tau^{2-\alpha},$$

in which $a_m = (m+1)^{1-\alpha} - m^{1-\alpha}$ and

$${}^C\mathcal{P}_t^\alpha(v(t)) = \frac{\tau^{-1}}{\Gamma(2-\alpha)}\left[a_0 v(t_k) - \sum_{m=1}^{k-1}(a_{k-m-1}\right.$$

$$\left. - a_{k-m})v(t_m) - a_{k-1}v(t_0) \right].$$

Lemma 2.3 [40] *For any $\mathcal{Q} = \left\{\mathcal{Q}_1, \mathcal{Q}_2, \dots \mathcal{Q}_N\right\}$ and q, we obtain*

$$\sum_{n=1}^{N}\left[a_0\mathcal{Q}_n - \sum_{k=1}^{n-1}\left(a_{n-k-1} - a_{n-k}\right)\mathcal{Q}_k - a_{n-1}q\right]\mathcal{Q}_n$$

$$\ge \frac{t_N^{-\alpha}}{2}\tau\sum_{n=1}^{N}\mathcal{Q}_n^2 - \frac{t_N^{1-\alpha}}{2(2-\alpha)}q^2, \quad N = 1, 2, 3, \dots.$$

Let

$$\vartheta^\alpha(x, y, t) = \frac{1}{\Gamma(1-\alpha)}\int_0^t \frac{\partial u(x, y, s)}{\partial s}\frac{\mathrm{d}s}{(t-s)^\alpha}.$$

(5)

Then Eq. (1) can be written as follows:

$$\int_0^1 w(\alpha)\vartheta^\alpha(x, y, t)\mathrm{d}\alpha = \Delta u(x, y, t) - v \cdot \nabla u(x, y, t)$$

$$+ f(x, y, t), \quad (x, y) \in \Omega, \quad 0 < t \le T.$$

(6)

If we set

$$\mathcal{J}(\alpha, x, y, t) = w(\alpha)\vartheta^{\alpha}(x, y, t), \tag{7}$$

then

$$\int_0^1 \mathcal{J}(\alpha, \mathbf{x}, t)\mathrm{d}\alpha = \Delta u(\mathbf{x}, t) - v \cdot \nabla u(\mathbf{x}, t) + f(\mathbf{x}, t). \tag{8}$$

Applying Lemma 2.1, we get

$$
\begin{aligned}
&\int_0^1 \mathcal{J}(\alpha, x, y, t)\mathrm{d}\alpha \\
&= \sum_{l=0}^{N_q} \omega_l \mathcal{J}(\alpha_l, x, y, t) - \mathrm{e}_n \left. \frac{\mathcal{J}^{(2n)}(\alpha, x, y, t)}{(2n)!}\right|_{\alpha=\eta} \\
&= \sum_{l=0}^{N_q} \omega_l \mathcal{J}(\alpha_l, x, y, t) + \mathcal{R}_{\text{Gauss}} \\
&= \sum_{l=0}^{N_q} \omega_l w(\alpha_l)\vartheta^{\alpha_l}(x, y, t) + \mathcal{R}_{\alpha}^{n-\frac{1}{2}},
\end{aligned} \tag{9}
$$

in which

$$
\begin{aligned}
\mathcal{R}_{Gauss} &= -\mathrm{e}_n \left. \frac{\mathcal{J}^{(2n)}(\alpha, x, y, t)}{(2n)!}\right|_{\alpha=\eta}, \\
\mathcal{R}_{\alpha}^{n-\frac{1}{2}} &= \mathcal{R}_{Gauss} + h_{\alpha} \sum_{l=0}^{N_q} \omega_l w(\alpha_l)\mathcal{R}_1^{\alpha_l},
\end{aligned} \tag{10}
$$

and also

$$\mathcal{R}_1^{\alpha_l} = C_{\alpha_l} \max_{0 \le t \le t_n} \left| \frac{\partial^2 v(x, y, t)}{\partial t^2} \right| \tau^{3-\alpha_l}.$$

At this moment, we know

$$\left|\mathcal{R}_{Gauss}\right| \le C_1 \mathrm{e}_n, \quad \left|\mathcal{R}_1^{\alpha_l}\right| \le C_2 \tau^{3-\alpha_l}, \tag{11}$$

then we have

$$
\begin{aligned}
\left|\mathcal{R}_{\alpha}^{n-\frac{1}{2}}\right| &= \left|\mathcal{R}_{Gauss} - \sum_{l=0}^{N_q} \omega_l w(\alpha_l)\mathcal{R}_1^{\alpha_l}\right| \\
&\le \left|\mathcal{R}_{Gauss}\right| + \left|\sum_{l=0}^{N_q} \omega_l w(\alpha_l)\mathcal{R}_1^{\alpha_l}\right| \le C(\mathrm{e}_n + \tau^{1+\frac{1}{2N_q}}).
\end{aligned} \tag{12}
$$

Now, substituting (9) in (8), we obtain

$$\sum_{l=0}^{N_q} \omega_l w(\alpha_l)\vartheta^{\alpha_l} + \mathcal{R}_{\text{Gauss}} = \Delta u - v \cdot \nabla u + f + \mathcal{E}_{\alpha}^{n-\frac{1}{2}}, \tag{13}$$

as Lemma 2.2 gives

$$
\begin{aligned}
&\sum_{l=0}^{N_q} \left\{ \omega_l w(\alpha_l)\frac{1}{\Gamma(2-\alpha_l)\tau}\left\{ a_0^{\alpha_l}u^{n-\frac{1}{2}} - \sum_{k=1}^{n-1}\left(a_{n-k-1}^{\alpha_l} \right.\right.\right. \\
&\left.\left.\left. -a_{n-k}^{\alpha_l}\right)u^{k-\frac{1}{2}} - a_{n-1}^{\alpha_l}\varphi \right\}\right\} \\
&= \Delta u(x, y, t_{n-\frac{1}{2}}) - v \cdot \nabla u(x, y, t_{n-\frac{1}{2}}) \\
&\quad + f(x, y, t_{n-\frac{1}{2}}) + \mathcal{E}_{\alpha}^{n-\frac{1}{2}},
\end{aligned} \tag{14}
$$

in which there exists a positive constant C such that

$$\mathcal{E}_{\alpha}^{n-\frac{1}{2}} < C\tau^{3-\alpha_{max}}. \tag{15}$$

Omitting the small term $\mathcal{E}_{\alpha}^{n-\frac{1}{2}}$ in Eq. (14), we can get

$$
\begin{aligned}
&\sum_{l=0}^{N_q} \left\{ \omega_l w(\alpha_l)\frac{1}{\Gamma(2-\alpha_l)\tau}\left\{ a_0^{\alpha_l}U^{n-\frac{1}{2}} - \sum_{k=1}^{n-1}\left(a_{n-k-1}^{\alpha_l} \right.\right.\right. \\
&\left.\left.\left. -a_{n-k}^{\alpha_l}\right)U^{k-\frac{1}{2}} - a_{n-1}^{\alpha_l}\varphi \right\}\right\} \\
&= \Delta U^{n-\frac{1}{2}} - v \cdot \nabla U^{n-\frac{1}{2}} + f(x, y, t_{n-\frac{1}{2}}).
\end{aligned} \tag{16}
$$

2.1 Stability and convergence of the semi-discrete scheme

In the current section, we study the stability and convergence of the time-discrete scheme.

Theorem 2.4 *Let $U^n \in H_0^1(\Omega)$. Then difference scheme* (16) *is unconditionally stable.*

Proof Multiplying both sides of Eq. (16) by $U^{n-\frac{1}{2}}$ and integrating on Ω give

$$
\begin{aligned}
&\sum_{l=0}^{N_q} \left\{ \omega_l w(\alpha_l)\frac{1}{\Gamma(2-\alpha_l)\tau}\left\{ a_0^{\alpha_l}\left\|U^{n-\frac{1}{2}}\right\|_{L^2(\Omega)}^2 - \sum_{k=1}^{n-1}\left(a_{n-k-1}^{\alpha_l}\right.\right.\right. \\
&\left.\left.\left. -a_{n-k}^{\alpha_l}\right)\left(U^{k-\frac{1}{2}}, U^{n-\frac{1}{2}}\right) - a_{n-1}^{\alpha_l}\left(\varphi, U^{n-\frac{1}{2}}\right) \right\}\right\} \\
&= \left(\Delta U^{n-\frac{1}{2}}, U^{n-\frac{1}{2}}\right) - \left(v \cdot \nabla U^{n-\frac{1}{2}}, U^{n-\frac{1}{2}}\right) \\
&\quad + \left(f(x, y, t_{n-\frac{1}{2}}), U^{n-\frac{1}{2}}\right).
\end{aligned} \tag{17}
$$

By simplification the above relation, we can get

$$
\sum_{l=0}^{N_q} \left\{ \frac{\omega_l w(\alpha_l)}{\Gamma(2-\alpha_l)\tau} \left\{ a_0^{\alpha_l} \left\| U^{n-\frac{1}{2}} \right\|_{L^2(\Omega)} - \sum_{k=1}^{n-1} \left(a_{n-k-1}^{\alpha_l} \right. \right. \right.
$$
$$
\left. \left. \left. - a_{n-k}^{\alpha_l} \right) \left\| U^{k-\frac{1}{2}} \right\|_{L^2(\Omega)} - a_{n-1}^{\alpha_l} \|\varphi\|_{L^2(\Omega)} \right\} \right\} \left\| U^{n-\frac{1}{2}} \right\|_{L^2(\Omega)}
$$
$$
+ \left\| \nabla U^{n-\frac{1}{2}} \right\|_{L^2(\Omega)}^2 \le -\left(v \cdot \nabla U^{n-\frac{1}{2}}, U^{n-\frac{1}{2}} \right)
$$
$$
+ \left(f(x,y,t_{n-\frac{1}{2}}), U^{n-\frac{1}{2}} \right). \tag{18}
$$

Applying Lemma 2.3 for the left-hand side of Eq. (18), results

$$
\sum_{l=0}^{N_q} \omega_l w(\alpha_l) \left\{ \frac{t_N^{-\alpha_l}}{2\Gamma(2-\alpha_l)} \sum_{n=1}^{N} \left\| U^{n-\frac{1}{2}} \right\|_{L^2(\Omega)}^2 \right.
$$
$$
\left. - \frac{t_N^{1-\alpha_l}}{\Gamma(2-\alpha_l)(1-\alpha_l)} \|\varphi\|_{L^2(\Omega)}^2 \right\}
$$
$$
+ \sum_{n=1}^{N} \left\| \nabla U^{n-\frac{1}{2}} \right\|_{L^2(\Omega)}^2 \le -\sum_{n=1}^{N} \left(v \cdot \nabla U^{n-\frac{1}{2}}, U^{n-\frac{1}{2}} \right)
$$
$$
+ \sum_{n=1}^{N} \left(f\left(x,y,t_{n-\frac{1}{2}}\right), U^{n-\frac{1}{2}} \right). \tag{19}
$$

The Cauchy–Schwarz and Young's inequalities, yield

$$
\sum_{l=0}^{N_q} \sum_{n=1}^{N} \frac{\omega_l w(\alpha_l) t_N^{-\alpha_l}}{2\Gamma(2-\alpha_l)} \left\| U^{n-\frac{1}{2}} \right\|_{L^2(\Omega)}^2
$$
$$
- \sum_{l=0}^{N_q} \frac{\omega_l w(\alpha_l) t_N^{1-\alpha_l}}{\Gamma(2-\alpha_l)(1-\alpha_l)} \|\varphi\|_{L^2(\Omega)}^2
$$
$$
+ \sum_{n=1}^{N} \left\| \nabla U^{n-\frac{1}{2}} \right\|_{L^2(\Omega)}^2 \le \sum_{l=0}^{N_q} \sum_{n=1}^{N} \frac{\Gamma(2-\alpha_l)}{\omega_l w(\alpha_l) t_N^{-\alpha_l}} \left\| v \cdot \nabla U^{n-\frac{1}{2}} \right\|_{L^2(\Omega)}^2
$$
$$
+ \sum_{l=0}^{N_q} \sum_{n=1}^{N} \frac{\omega_l w(\alpha_l) t_N^{-\alpha_l}}{4\Gamma(2-\alpha_l)} \left\| U^{n-\frac{1}{2}} \right\|_{L^2(\Omega)}^2
$$
$$
+ \sum_{l=0}^{N_q} \sum_{n=1}^{N} \frac{\Gamma(2-\alpha_l)}{\omega_l w(\alpha_l) t_N^{-\alpha_l}} \left\| f^{n-\frac{1}{2}} \right\|_{L^2(\Omega)}^2
$$
$$
+ \sum_{l=0}^{N_q} \sum_{n=1}^{N} \frac{\omega_l w(\alpha_l) t_N^{-\alpha_l}}{4\Gamma(2-\alpha_l)} \left\| U^{n-\frac{1}{2}} \right\|_{L^2(\Omega)}^2. \tag{20}
$$

After simplification the above inequality, we can write

$$
\sum_{n=1}^{N} \left\| \nabla U^{n-\frac{1}{2}} \right\|_{L^2(\Omega)}^2
$$
$$
\le \sum_{l=0}^{N_q} \sum_{n=1}^{N} \frac{\Gamma(2-\alpha_l)}{\omega_l w(\alpha_l) t_N^{-\alpha_l}} \left\| v \cdot \nabla U^{n-\frac{1}{2}} \right\|_{L^2(\Omega)}^2
$$
$$
+ \sum_{l=0}^{N_q} \sum_{n=1}^{N} \frac{\Gamma(2-\alpha_l)}{\omega_l w(\alpha_l) t_N^{-\alpha_l}} \left\| f^{n-\frac{1}{2}} \right\|_{L^2(\Omega)}^2
$$
$$
+ \sum_{l=0}^{N_q} \frac{\omega_l w(\alpha_l) t_N^{1-\alpha_l}}{\Gamma(2-\alpha_l)(1-\alpha_l)} \|\varphi\|_{L^2(\Omega)}^2, \tag{21}
$$

or equivalently

$$
\left\| \nabla U^{n-\frac{1}{2}} \right\|_{L^2(\Omega)}^2 \le \sum_{l=0}^{N_q} \sum_{j=1}^{n} \frac{\Gamma(2-\alpha_l)}{\omega_l w(\alpha_l) t_n^{-\alpha_l}} \left\| v \cdot \nabla U^{j-\frac{1}{2}} \right\|_{L^2(\Omega)}^2
$$
$$
+ \sum_{l=0}^{N_q} \sum_{j=1}^{n} \frac{\Gamma(2-\alpha_l)}{\omega_l w(\alpha_l) t_n^{-\alpha_l}} \left\| f^{j-\frac{1}{2}} \right\|_{L^2(\Omega)}^2
$$
$$
+ \sum_{l=0}^{N_q} \frac{\omega_l w(\alpha_l) t_n^{1-\alpha_l}}{\Gamma(2-\alpha_l)(1-\alpha_l)} \|\varphi\|_{L^2(\Omega)}^2. \tag{22}
$$

The use of Grönwall's inequality, gives

$$
\left\| \nabla U^{n-\frac{1}{2}} \right\|_{L^2(\Omega)}^2
$$
$$
\le \left[\sum_{l=0}^{N_q} \sum_{j=1}^{n} \frac{\Gamma(2-\alpha_l)}{\omega_l w(\alpha_l) t_n^{-\alpha_l}} \left\| f^{j-\frac{1}{2}} \right\|_{L^2(\Omega)}^2 \right.
$$
$$
\left. + \sum_{l=0}^{N_q} \frac{\omega_l w(\alpha_l) t_n^{1-\alpha_l}}{\Gamma(2-\alpha_l)(1-\alpha_l)} \|\varphi\|_{L^2(\Omega)}^2 \right] \exp \left(\sum_{l=0}^{N_q} \frac{v\Gamma(2-\alpha_l)}{\omega_l w(\alpha_l)} \sum_{j=1}^{n} t_n^{\alpha_l} \right)
$$
$$
\le \left[\sum_{l=0}^{N_q} \sum_{j=1}^{n} \frac{\Gamma(2-\alpha_l)}{\omega_l w(\alpha_l) t_n^{-\alpha_l}} \left\| f^{j-\frac{1}{2}} \right\|_{L^2(\Omega)}^2 \right.
$$
$$
\left. + \sum_{l=0}^{N_q} \frac{\omega_l w(\alpha_l) t_n^{1-\alpha_l}}{\Gamma(2-\alpha_l)(1-\alpha_l)} \|\varphi\|_{L^2(\Omega)}^2 \right] \exp \left(\sum_{l=0}^{N_q} \frac{v\Gamma(2-\alpha_l)}{\omega_l w(\alpha_l)} \frac{n\tau}{1-n\tau} \right), \tag{23}
$$

also, using the Poincare inequality we can get the following relation:

$$\left\|U^{n-\frac{1}{2}}\right\|_{L^2(\Omega)}^2 \leq C_\Omega \left\|\nabla U^{n-\frac{1}{2}}\right\|_{L^2(\Omega)}^2$$

$$\leq C \left[\sum_{l=0}^{N_q} \sum_{j=1}^{n} \frac{\Gamma(2-\alpha_l)}{\omega_l w(\alpha_l) t_n^{-\alpha_l}} \left\|f^{j-\frac{1}{2}}\right\|_{L^2(\Omega)}^2 \right.$$

$$\left. + \sum_{l=0}^{N_q} \frac{\omega_l w(\alpha_l) t_n^{1-\alpha_l}}{\Gamma(2-\alpha_l)(1-\alpha_l)} \|\varphi\|_{L^2(\Omega)}^2 \right]. \tag{24}$$

Finally, we have the following inequality:

$$\left\|U^{n-\frac{1}{2}}\right\|_{L^2(\Omega)} \leq C_\Omega \left[\sum_{l=0}^{N_q} \sum_{j=1}^{n} \frac{\Gamma(2-\alpha_l)}{\omega_l w(\alpha_l) t_n^{-\alpha_l}} \left\|f^{j-\frac{1}{2}}\right\|_{L^2(\Omega)} \right.$$

$$\left. + \sum_{l=0}^{N_q} \frac{\omega_l w(\alpha_l) t_n^{1-\alpha_l}}{\Gamma(2-\alpha_l)(1-\alpha_l)} \|\varphi\|_{L^2(\Omega)} \right], \tag{25}$$

which completes the proof. □

Theorem 2.5 *Let u^n and U^n be solutions of Eqs.* (14) *and* (16), *respectively, and they belong to $H_0^1(\Omega)$. Then, difference scheme* (16) *is convergent with convergence order $O(\tau^{\frac{3}{2}})$.*

Proof We define the following notation:

$\Phi^n = u^n - U^n$.
Subtracting Eq. (16) from Eq. (14), gives

$$\sum_{l=0}^{N_q} \left\{ \omega_l w(\alpha_l) \frac{1}{\Gamma(2-\alpha_l)\tau} \left\{ a_0^{\alpha_l} \Phi^{n-\frac{1}{2}} - \sum_{k=1}^{n-1} \left(a_{n-k-1}^{\alpha_l} \right. \right. \right.$$

$$\left. \left. \left. - a_{n-k}^{\alpha_l}\right)\Phi^{k-\frac{1}{2}} \right\} \right\} = \Delta\Phi^{n-\frac{1}{2}} - v\cdot\nabla\Phi^{n-\frac{1}{2}} + \mathcal{E}_\alpha^{n-\frac{1}{2}}. \tag{26}$$

Multiplying both sides of Eq. (26) by $\Phi^{n-\frac{1}{2}}$ and integrating on Ω result in

$$\sum_{l=0}^{N_q} \left\{ \omega_l w(\alpha_l) \frac{1}{\Gamma(2-\alpha_l)\tau} \left\{ a_0^{\alpha_l} \left\|\Phi^{n-\frac{1}{2}}\right\|_{L^2(\Omega)}^2 \right. \right.$$

$$\left. \left. - \sum_{k=1}^{n-1} \left(a_{n-k-1}^{\alpha_l} - a_{n-k}^{\alpha_l}\right)\left(\Phi^{k-\frac{1}{2}}, \Phi^{n-\frac{1}{2}}\right) \right\} \right\}$$

$$= -\left(\nabla\Phi^{n-\frac{1}{2}}, \nabla\Phi^{n-\frac{1}{2}}\right) - \left(v\cdot\nabla\Phi^{n-\frac{1}{2}}, \Phi^{n-\frac{1}{2}}\right)$$

$$+ \left(\mathcal{E}_\alpha^{n-\frac{1}{2}}, \Phi^{n-\frac{1}{2}}\right), \tag{27}$$

and also, we can get

$$\sum_{l=0}^{N_q} \left\{ \omega_l w(\alpha_l) \frac{1}{\Gamma(2-\alpha_l)\tau} \left\{ a_0^{\alpha_l} \left\|\Phi^{n-\frac{1}{2}}\right\|_{L^2(\Omega)} \right. \right.$$

$$\left. \left. - \sum_{k=1}^{n-1} \left(a_{n-k-1}^{\alpha_l} - a_{n-k}^{\alpha_l}\right)\left\|\Phi^{k-\frac{1}{2}}\right\|_{L^2(\Omega)} \right\} \right\} \left\|\Phi^{n-\frac{1}{2}}\right\|_{L^2(\Omega)}$$

$$+ \left\|\nabla\Phi^{n-\frac{1}{2}}\right\|_{L^2(\Omega)}^2 \leq \left\|v\cdot\nabla\Phi^{n-\frac{1}{2}}\right\|_{L^2(\Omega)}\left\|\Phi^{n-\frac{1}{2}}\right\|_{L^2(\Omega)}$$

$$+ \left(\mathcal{E}_\alpha^{n-\frac{1}{2}}, \Phi^{n-\frac{1}{2}}\right). \tag{28}$$

Summing the above relation for n from $n = 1$ to $n = N$ results in

$$\sum_{l=0}^{N_q} \left\{ \omega_l w(\alpha_l) \frac{1}{\Gamma(2-\alpha_l)\tau} \sum_{n=1}^{N} \left\{ a_0^{\alpha_l} \left\|\Phi^{n-\frac{1}{2}}\right\|_{L^2(\Omega)} \right. \right.$$

$$\left. \left. - \sum_{k=1}^{n-1} \left(a_{n-k-1}^{\alpha_l} - a_{n-k}^{\alpha_l}\right)\left\|\Phi^{k-\frac{1}{2}}\right\|_{L^2(\Omega)} \right\} \right\} \left\|\Phi^{n-\frac{1}{2}}\right\|_{L^2(\Omega)}$$

$$+ \sum_{n=1}^{N} \left\|\nabla\Phi^{n-\frac{1}{2}}\right\|_{L^2(\Omega)}^2 \leq \sum_{n=1}^{N} \left\|v\cdot\nabla\Phi^{n-\frac{1}{2}}\right\|_{L^2(\Omega)}\left\|\Phi^{n-\frac{1}{2}}\right\|_{L^2(\Omega)}$$

$$+ \sum_{n=1}^{N} \left(\mathcal{E}_\alpha^{n-\frac{1}{2}}, \Phi^{n-\frac{1}{2}}\right). \tag{29}$$

Employing Lemma 2.3 for the left-hand side of Eq. (29) gives

$$\sum_{l=0}^{N_q} \sum_{n=1}^{N} \frac{\omega_l w(\alpha_l) t_N^{-\alpha_l}}{2\Gamma(2-\alpha_l)} \left\|\Phi^{n-\frac{1}{2}}\right\|_{L^2(\Omega)}^2 + \sum_{n=1}^{N} \left\|\nabla\Phi^{n-\frac{1}{2}}\right\|_{L^2(\Omega)}^2$$

$$\leq \sum_{l=0}^{N_q} \left\{ \omega_l w(\alpha_l) \frac{1}{\Gamma(2-\alpha_l)\tau} \sum_{n=1}^{N} \left\{ a_0^{\alpha_l} \left\|\Phi^{n-\frac{1}{2}}\right\|_{L^2(\Omega)} \right. \right.$$

$$\left. \left. - \sum_{k=1}^{n-1} \left(a_{n-k-1}^{\alpha_l} - a_{n-k}^{\alpha_l}\right)\left\|\Phi^{k-\frac{1}{2}}\right\|_{L^2(\Omega)} \right\} \right\} \left\|\Phi^{n-\frac{1}{2}}\right\|_{L^2(\Omega)}$$

$$+ \sum_{n=1}^{N} \left\|\nabla\Phi^{n-\frac{1}{2}}\right\|_{L^2(\Omega)}^2 \leq \sum_{n=1}^{N} \left\|v\cdot\nabla\Phi^{n-\frac{1}{2}}\right\|_{L^2(\Omega)}\left\|\Phi^{n-\frac{1}{2}}\right\|_{L^2(\Omega)}$$

$$+ \sum_{n=1}^{N} \left(\mathcal{E}_\alpha^{n-\frac{1}{2}}, \Phi^{n-\frac{1}{2}}\right). \tag{30}$$

Using the Cauchy–Schwarz and Young's inequalities, the following relation can be constructed:

$$\sum_{l=0}^{N_q}\sum_{n=1}^{N}\frac{\omega_l w(\alpha_l)t_N^{-\alpha_l}}{2\Gamma(2-\alpha_l)}\left\|\Phi^{n-\frac{1}{2}}\right\|_{L^2(\Omega)}^2 + \sum_{n=1}^{N}\left\|\nabla\Phi^{n-\frac{1}{2}}\right\|_{L^2(\Omega)}^2$$

$$\leq \sum_{n=1}^{N}\frac{2\Gamma(2-\alpha_l)}{\omega_l w(\alpha_l)t_N^{-\alpha_l}}\left\|v\cdot\nabla\Phi^{n-\frac{1}{2}}\right\|_{L^2(\Omega)}^2$$

$$+\sum_{l=0}^{N_q}\sum_{n=1}^{N}\frac{\omega_l w(\alpha_l)t_N^{-\alpha_l}}{4\Gamma(2-\alpha_l)}\left\|\Phi^{n-\frac{1}{2}}\right\|_{L^2(\Omega)}^2 \qquad (31)$$

$$+\sum_{l=0}^{N_q}\sum_{n=1}^{N}\frac{2\Gamma(2-\alpha_l)}{\omega_l w(\alpha_l)t_N^{-\alpha_l}}\left\|\mathcal{E}_\alpha^{n-\frac{1}{2}}\right\|_{L^2(\Omega)}^2$$

$$+\sum_{l=0}^{N_q}\sum_{n=1}^{N}\frac{\omega_l w(\alpha_l)t_N^{-\alpha_l}}{4\Gamma(2-\alpha_l)}\left\|\Phi^{n-\frac{1}{2}}\right\|_{L^2(\Omega)}^2.$$

Simplifying the above relation yields

$$\sum_{n=1}^{N}\left\|\nabla\Phi^{n-\frac{1}{2}}\right\|_{L^2(\Omega)}^2 \leq \sum_{n=1}^{N}\frac{2v\Gamma(2-\alpha_l)}{\omega_l w(\alpha_l)t_N^{-\alpha_l}}\left\|\nabla\Phi^{n-\frac{1}{2}}\right\|_{L^2(\Omega)}^2$$

$$+\sum_{l=0}^{N_q}\sum_{n=1}^{N}\frac{2\Gamma(2-\alpha_l)}{\omega_l w(\alpha_l)t_N^{-\alpha_l}}\left\|\mathcal{E}_\alpha^{n-\frac{1}{2}}\right\|_{L^2(\Omega)}^2, \qquad (32)$$

or equivalently

$$\left\|\nabla\Phi^{n-\frac{1}{2}}\right\|_{L^2(\Omega)}^2 \leq \sum_{j=1}^{n}\left\|\nabla\Phi^{j-\frac{1}{2}}\right\|_{L^2(\Omega)}^2$$

$$\leq \sum_{j=1}^{n}\frac{2v\Gamma(2-\alpha_l)}{\omega_l w(\alpha_l)t_N^{-\alpha_l}}\left\|\nabla\Phi^{j-\frac{1}{2}}\right\|_{L^2(\Omega)}^2 \qquad (33)$$

$$+\sum_{l=0}^{N_q}\sum_{j=1}^{n}\frac{2\Gamma(2-\alpha_l)}{\omega_l w(\alpha_l)t_n^{-\alpha_l}}\left\|\mathcal{E}_\alpha^{j-\frac{1}{2}}\right\|_{L^2(\Omega)}^2.$$

From relation (15), we can conclude the following estimates:

$$\left\|\nabla\Phi^{n-\frac{1}{2}}\right\|_{L^2(\Omega)}^2 \leq \sum_{j=1}^{n}\left\|\nabla\Phi^{j-\frac{1}{2}}\right\|_{L^2(\Omega)}^2$$

$$\leq \sum_{j=1}^{n}\frac{2v\Gamma(2-\alpha_l)}{\omega_l w(\alpha_l)t_N^{-\alpha_l}}\left\|\nabla\Phi^{j-\frac{1}{2}}\right\|_{L^2(\Omega)}^2$$

$$+\sum_{l=0}^{N_q}\sum_{j=1}^{n}\frac{2\Gamma(2-\alpha_l)}{\omega_l w(\alpha_l)t_n^{-\alpha_l}}\left\|\mathcal{E}_\alpha^{j-\frac{1}{2}}\right\|_{L^2(\Omega)}^2$$

$$\leq \sum_{j=1}^{n}\frac{2v\Gamma(2-\alpha_l)}{\omega_l w(\alpha_l)t_N^{-\alpha_l}}\left\|\nabla\Phi^{j-\frac{1}{2}}\right\|_{L^2(\Omega)}^2 \qquad (34)$$

$$+\sum_{l=0}^{N_q}\frac{2C\left(\tau^{3-\alpha_{max}}\right)^2\Gamma(2-\alpha_l)}{\omega_l w(\alpha_l)t_n^{-\alpha_l}}$$

$$\leq \sum_{j=1}^{n}\frac{2v\Gamma(2-\alpha_l)}{\omega_l w(\alpha_l)t_N^{-\alpha_l}}\left\|\nabla\Phi^{j-\frac{1}{2}}\right\|_{L^2(\Omega)}^2$$

$$+ C(\alpha_{max},\omega)n\left(\tau^{3-\alpha_{max}}\right)^2.$$

Multiplying τ on both sides of the above relation and applying the Grönwall's inequality, we arrive at

$$\tau\left\|\nabla\Phi^{n-\frac{1}{2}}\right\|_{L^2(\Omega)}^2$$

$$\leq \tau\sum_{j=1}^{n}\frac{2v\Gamma(2-\alpha_l)}{\omega_l w(\alpha_l)t_n^{-\alpha_l}}\left\|\nabla\Phi^{j-\frac{1}{2}}\right\|_{L^2(\Omega)}^2$$

$$+ C(\alpha_{max},\omega)T\left(\tau^{3-\alpha_{max}}\right)^2 \qquad (35)$$

$$\leq C(\alpha_{max},\omega)T\left(\tau^{3-\alpha_{max}}\right)^2\exp\left(\tau\sum_{j=1}^{n}\frac{2v\Gamma(2-\alpha_l)}{\omega_l w(\alpha_l)t_n^{-\alpha_l}}\right)$$

$$\leq C^*(\alpha_{max},\omega)T\left(\tau^{3-\alpha_{max}}\right)^2.$$

Finally, we can obtain the following bound:

$$\tau\left\|\Phi^{n-\frac{1}{2}}\right\|_{L^2(\Omega)} \leq \sqrt{C^*(\alpha_{max},\omega)T}\,\tau^{3-\alpha_{max}}. \qquad (36)$$

$\square$

3 Radial basis function approximation

The main advantage of the mesh-free methods is that they are not dependent on any mesh or element. The mesh-free methods are related to a set of scattered data points. Thus, we can consider any geometry as a computational domain. One of the mesh-free techniques is the RBF collocation procedure. Thus, we explain some basic concepts.
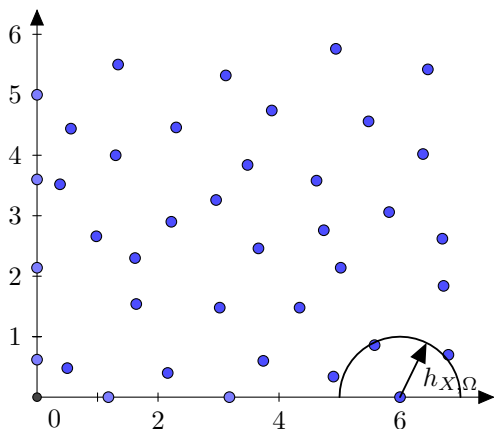
Definition 3.1 [42] A symmetric function $\phi \in \mathbb{R}^d \times \mathbb{R}^d \longrightarrow \mathbb{R}$ is so-called strictly conditionally positive definite of order m, if for all sets $X = \{x_1, \ldots, x_N\} \subset \mathbb{R}^d$, and all vectors $c \in \mathbb{R}^d$ satisfying

$$\sum_{i=1}^{N} c_i p(x_i) = 0,$$

as for $p \in \mathbb{P}_{m-1}^d$

$$c^T A c = \sum_{i=1}^{N} \sum_{j=1}^{N} c_i \lambda_j \phi(x_i - x_j),$$

is positive, whenever $c \neq 0$.

Let ϕ be a strictly conditionally positive definite of order m, then the interpolation of a continuous function $f : \mathbb{R}^d \longrightarrow \mathbb{R}$ on a set $X = \{x_1, \ldots, x_N\}$ is

$$\mathcal{P}f(x) = \sum_{i=1}^{N} c_i \phi(x - x_i) + \sum_{j=1}^{l} \eta_j p_j(x),$$

such as $l = \binom{d + m - 1}{m - 1}$ and $\{p_1, p_2, \ldots, p_l\}$ is a basis of $\mathbb{P}_{m-1}^d$. We want to find $N + l$ unknown coefficients c_i and η_j as

$$\mathcal{P}f(x_i) = f_i, \quad i = 1, \ldots, N,$$

and

$$\sum_{i=1}^{N} c_i p_j(x_i) = 0, \quad 1 \leq j \leq l.$$

Definition 3.2 [42] The density of X in Ω is the number

$$h = h_{X,\Omega} = \sup_{x \in \Omega} \min_{x_j \in X} \left\| x - x_j \right\|.$$

3.1 Preliminary for local meshless collocation method

The local interpolation concept is as follows: [23, 24]

$$\mathcal{P}_m f(x) = \sum_{j \in \mathcal{I}_i} \vec{\lambda}_j \phi\left(\left\| x - y_j \right\|\right), \tag{37}$$

in which

1. y is a set of center points,
2. $\mathcal{I}_i$ is support domain of ith node,
3. $\vec{\lambda}$ is the unknown coefficient that must be calculated.

Employing the interpolation condition yields [23, 24]

$$\mathcal{P}_m f(x_j) = f(x_j). \tag{38}$$

The vector-matrix form of Eq. (38) is

$$\mathbf{M}\vec{\lambda} = \mathbf{F}, \tag{39}$$

in which

- $\mathbf{F} = \left[f(x_1), f(x_2), \ldots, f(x_{|\mathcal{I}_i|}) \right]^T$,
- $\mathbf{M}_{jk} = \phi\left(\left\| x_j - x_k \right\|_2\right), \quad j, k \in \mathcal{I}_i$.

The local RBF operator can be introduced [23, 24]

$$\mathcal{L}f(x) = \sum_{j \in \mathcal{I}_i} \lambda_j \mathcal{L}\psi\left(\left\| x - y_j \right\|_2\right). \tag{40}$$

Also, we can write

$$\mathcal{L}f(x) = \Lambda^T \vec{\lambda}, \tag{41}$$

in which

$$(\Lambda)_i = \phi\left(\left\| x - y_i \right\|_2\right), \quad i \in \mathcal{I}_i. \tag{42}$$

Thus, Eqs. (39) and (41) result [23, 24]

$$\mathcal{L}f(\vec{x})\big|_{\mathcal{I}_i} = \left(\Lambda^T \mathbf{B}^{-1}\right)\mathbf{f}\big|_{\mathcal{I}_i} = (\vec{w}_i)\mathbf{f}, \tag{43}$$

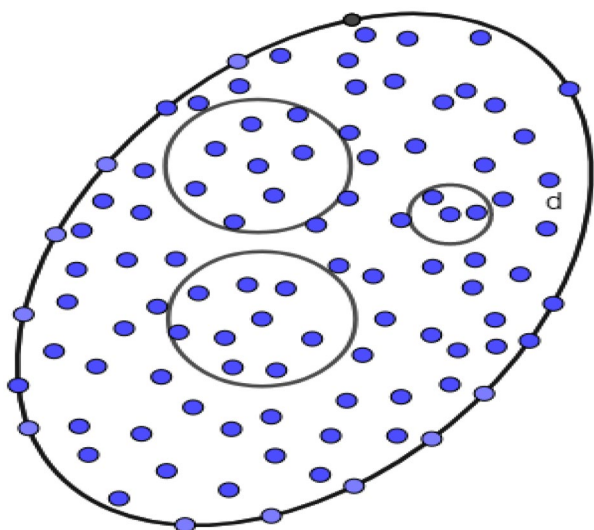in which $\vec{w}_i$ is the stencil weights at RBFs center i.

Fig. 1 Configuration in the local support

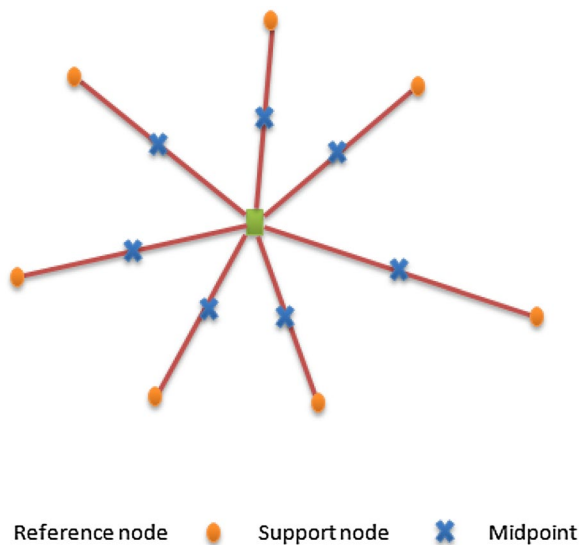Reference node   Support node   Midpoint

Fig. 2 Configuration in the local support

3.2 The meshless local RBF-FD (LRBF-FD) technique

Let arbitrary points $(x_i, y_i) \in \Omega$ be scattered in the computational domain $\bar{\Omega}$. We can consider a support domain including n_i nodes for each point $(x_i, y_i) \in \Omega$ as is depicted in Fig. 1. According to the previous section, the weight coefficients at each local domain can be calculated as

$$\left.\frac{\partial^m v(x, y)}{\partial x^m}\right|_{(x,y)=(x_i,y_i)} = \sum_{j=0}^{n_i} \rho_{i,j}^{m,x} v(x_j^i, y_j^i),$$

$$i = 0, 1, 2, \ldots, N. \tag{44}$$

Also, the mth derivative of RBFs at center point (x_i, y_i) is

$$\left.\frac{\partial^m \phi_j(x, y)}{\partial x^m}\right|_{(x,y)=(x_i,y_i)} = \sum_{p=0}^{n_i} \rho_{i,p}^{m,x} \phi_j(x_p^i, y_p^i),$$

$$i, j = \{0, 1, 2, \ldots, n_i\}, \quad i \neq j, \tag{45}$$

$$\left.\frac{\partial^m \phi_j(x, y)}{\partial y^m}\right|_{(x,y)=(x_i,y_i)} = \sum_{p=0}^{n_i} \rho_{i,p}^{m,y} \phi_j(x_p^i, y_p^i),$$

$$i, j = \{0, 1, 2, \ldots, n_i\}, \quad i \neq j, \tag{46}$$

where ϕ_j is a RBF. By collocating all nodes in the local domain of center point (x_i, y_i) in Eqs. (45) and (46), the following matrix equations have been resulted:

$$[\rho^{x,m}] = [A]^{-1} \left[\frac{\partial^m \phi(x_i, y_i)}{\partial x^m}\right],$$

$$[\rho^{y,m}] = [A]^{-1} \left[\frac{\partial^m \phi(x_i, y_i)}{\partial y^m}\right], \tag{47}$$

in which A is the interpolation matrix.

3.3 The upwind LRBFs-DQ approach

Shu et al. [39] developed a new version of LRBFs-DQ technique based on the upwind approach. We consider model (6) as follows:

$$_0^C D_t^\alpha \mathbf{U} + [\mathcal{M}(\mathbf{U}) - \mathcal{H}(\mathbf{U})]\mathbf{U}_x + [\mathcal{N}(\mathbf{U}) - \mathcal{J}(\mathbf{U})]\mathbf{U}_y = \mathbf{K}. \tag{48}$$

At first, we employ nodes between the center point and its support that are depicted in Fig. 2. Also, we call these points as the "*mid-points*".

Applying the LRBFs-DQ technique to discrete the space variable gives

$$_0^C D_t^\alpha \mathbf{U}_i = -\sum_{k=0}^{n_i} \left\{ \rho_{i,k}^{(x)} [\mathcal{M}(\mathbf{U}_{i,k}) - \mathcal{H}(\mathbf{U}_{i,k})] \right.$$

$$\left. + \rho_{i,k}^{(y)} [\mathcal{N}(\mathbf{U}_{i,k}) - \mathcal{J}(\mathbf{U}_{i,k})] \right\}^n + \mathbf{K}|_i^n, \tag{49}$$

where [39]

- $\mathbf{U}_{i,k}$ denotes the conservative variables at the mid-points,
- $\rho_{i,k}^{(x)}$ and $\rho_{i,k}^{(y)}$ are weight coefficients based on the first-order derivatives in the x- and y-directions, respectively,
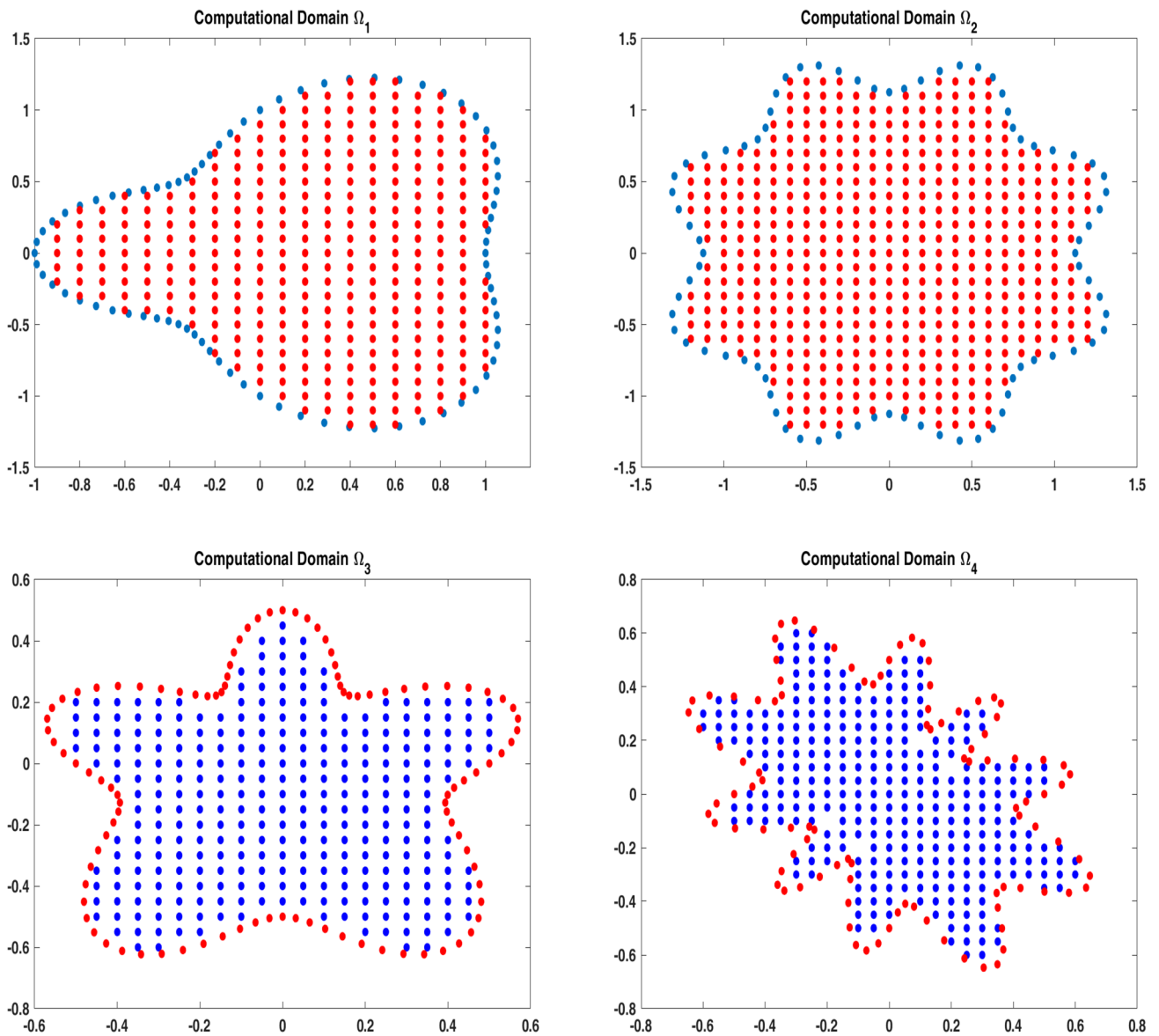- n_i denotes the total number of supporting points for the reference point i.

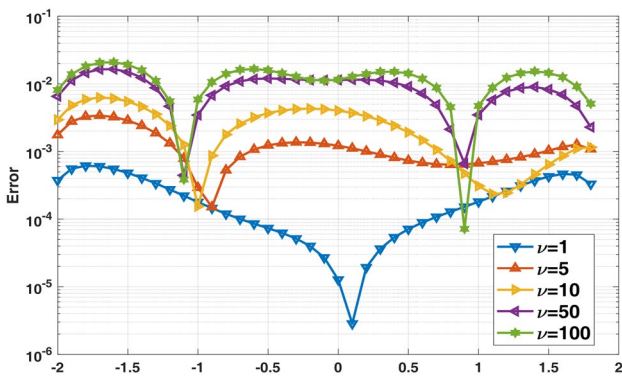**Fig. 3** The used computational regions

Fig. 4 Error obtained based on the values of ν on rectangular domain for Example 1

From Eq. (49), we can derive a new flux according to the mid-point and a unit vector

$$\vec{\alpha}_\rho = \left(\mu_{i,k}, \eta_{i,k} \right).$$

Thus, we have

$$
\begin{aligned}
\mathbf{S}_{i,k} =\, & \mu_{i,k} \left[\mathcal{M}(\mathbf{U}_{i,k}) - \mathcal{H}(\mathbf{U}_{i,k}) \right] \\
& + \eta_{i,k} \left[\mathcal{N}(\mathbf{U}_{i,k}) - \mathcal{J}(\mathbf{U}_{i,k}) \right],
\end{aligned}
\tag{50}
$$

in which [39]
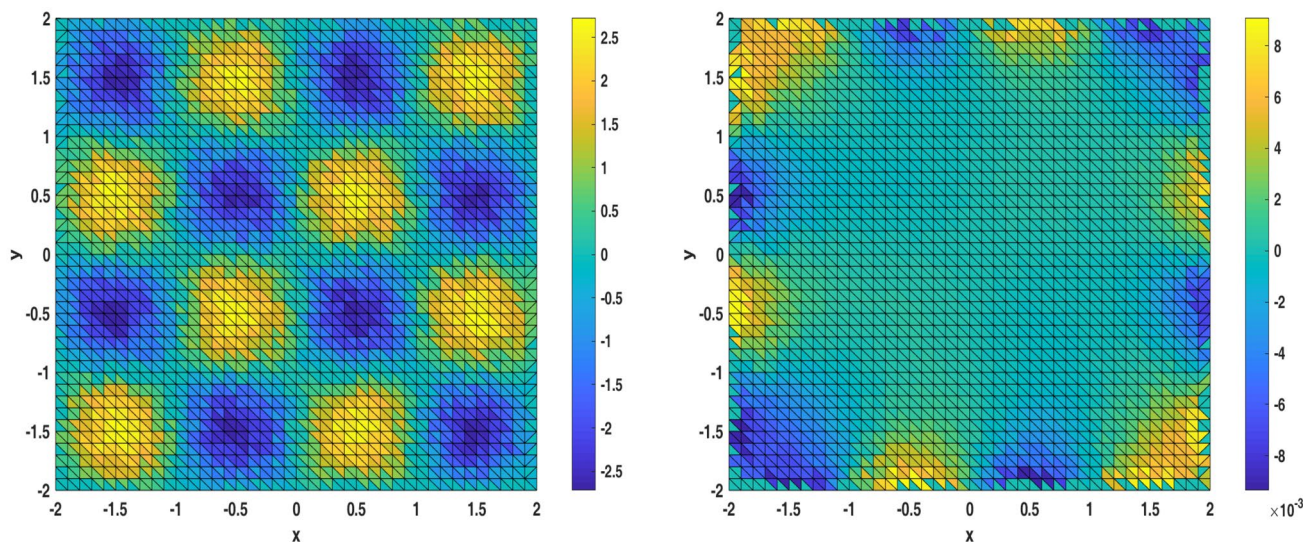
Fig. 5 Graph of approximate and error with $v = 10$ on rectangular domain for Example 1

Table 1 Errors obtained on rectangular domain for Example 1

N	$v = 1$	$v = 5$	$v = 10$	$v = 50$
20	8.2231×10^{-3}	2.3474×10^{-2}	5.5567×10^{-2}	9.3878×10^{-2}
40	2.4013×10^{-3}	8.6381×10^{-3}	1.0227×10^{-2}	4.2288×10^{-2}
60	6.5230×10^{-4}	2.3342×10^{-3}	7.2301×10^{-3}	1.2879×10^{-2}
80	1.0027×10^{-4}	7.8896×10^{-4}	1.4011×10^{-3}	7.3074×10^{-3}
120	7.2284×10^{-5}	3.0010×10^{-4}	8.4753×10^{-4}	1.8902×10^{-3}
150	2.1040×10^{-5}	9.0022×10^{-5}	2.1562×10^{-4}	8.8873×10^{-4}
200	8.5270×10^{-6}	4.5011×10^{-5}	9.4411×10^{-5}	2.0701×10^{-4}

Table 2 Errors obtained on domain Ω_2 for Example 1

N	$v = 1$	$v = 5$	$v = 10$	$v = 50$
20	3.2212×10^{-3}	7.7742×10^{-3}	2.3387×10^{-2}	8.3214×10^{-2}
40	8.0312×10^{-4}	2.2287×10^{-3}	8.9723×10^{-3}	1.0339×10^{-2}
60	2.1897×10^{-4}	7.9900×10^{-4}	3.0001×10^{-3}	7.6698×10^{-3}
80	7.6698×10^{-5}	1.9834×10^{-4}	7.8896×10^{-4}	2.8510×10^{-3}
120	2.0334×10^{-5}	8.7769×10^{-5}	1.2001×10^{-4}	7.9630×10^{-4}
150	9.7756×10^{-6}	1.3989×10^{-5}	7.5799×10^{-5}	2.0013×10^{-4}
200	3.5387×10^{-6}	9.0061×10^{-6}	3.0201×10^{-5}	9.8740×10^{-5}

$$\mu_{i,k} = \frac{\rho_{i,k}^{(x)}}{\sqrt{\left(\rho_{i,k}^{(x)}\right)^2 + \left(\rho_{i,k}^{(y)}\right)^2}},$$

$$\eta_{i,k} = \frac{\rho_{i,k}^{(y)}}{\sqrt{\left(\rho_{i,k}^{(x)}\right)^2 + \left(\rho_{i,k}^{(y)}\right)^2}}. \tag{51}$$

By assuming

$$\Theta_{i,k} = \sqrt{\left(\rho_{i,k}^{(x)}\right)^2 + \left(\rho_{i,k}^{(y)}\right)^2}. \tag{52}$$

Equation (49) can be rewritten as follows:

$$_0^C D_t^\alpha \mathbf{U}_i = -\sum_{k=0}^{N_1} \Theta_{i,k} \mathbf{S}_{i,k} + \mathbf{K}|_i. \tag{53}$$

4 Numerical surveys

Here, we report the obtained results based on the developed technique on the non-rectangular domains that are depicted in Fig. 3.

4.1 Example 1

We will study the following model:

$$\int_0^1 w(\alpha)_0^C D_t^\alpha u \, \mathrm{d}\alpha = \frac{\partial^2 u}{\partial x^2} + \frac{\partial^2 u}{\partial y^2} - v\frac{\partial u}{\partial x} - v\frac{\partial u}{\partial y} + f(x, y, t),$$

$$(54)$$

with the homogeneous initial and boundary conditions. Also, $w(\alpha) = \Gamma(3 - \alpha)$ and the analytical solution is

$$u(x, y, t) = \exp(-\pi^2 t) \sin(\pi x) \sin(\pi y);$$

thus, the source term can be obtained from the analytical solution. In this example, the effect of the advection coefficient has been studied. Figure 4 displays the error obtained based on the values of v on rectangular domain for Example 1. In Fig. 5, the graphs of approximate and error have been

depicted with $v = 10$ on rectangular domain for Example 1. Tables 1 and 2 show the errors obtained based on the different values of advection coefficient v with rectangular domain and domain Ω_2 for Example 1. Figures 7, 9, 11 and 13 demonstrate the approximation solutions based on the different computational geometries. Figures 6, 8, 10 and 12 illustrate error obtained based on the different values of and v for the computational domains Ω_1, Ω_2, Ω_3 and Ω_4, respectively.

4.2 Example 2

Consider the following model:

$$
\int_0^1 w(\alpha)\,{}_0^C D_t^\alpha u(x, y, t)\mathrm{d}\alpha = \frac{\partial^2 u(x, y, t)}{\partial x^2} + \frac{\partial^2 u(x, y, t)}{\partial y^2}
$$
$$
- v\frac{\partial u(x, y, t)}{\partial x} - v\frac{\partial u(x, y, t)}{\partial y} \tag{55}
$$
$$
+ f(x, y, t),
$$

with the homogeneous initial and boundary conditions. The analytical solution is

$$
u(x, y, t) = t^2(1 - x^2)^\sigma(1 - y^2)^\sigma,
$$

where σ is a positive constant as this solution belongs to Sobolev space $H_0^{\sigma+\frac{1}{2}}$ and also $w(\alpha) = \Gamma(3 - \alpha)$. Figure 14 demonstrates error obtained with $\sigma = 7/4$ and different values of v and also Fig. 15 illustrates error obtained with $v = 50$ and different values of σ for Example 2. Furthermore, Fig. 16 displays approximate solution with $v = 50$ and different values of σ for Example 2. Table 3 presents the error achieved based on the values of $\sigma = \frac{4}{3}$ and $\sigma = \frac{13}{3}$. According to these parameters, we choose different advection coefficients $v = 10$ and $v = 50$. In Table 3 the effect of the regularity solution and advection coefficient can be observed, clearly.
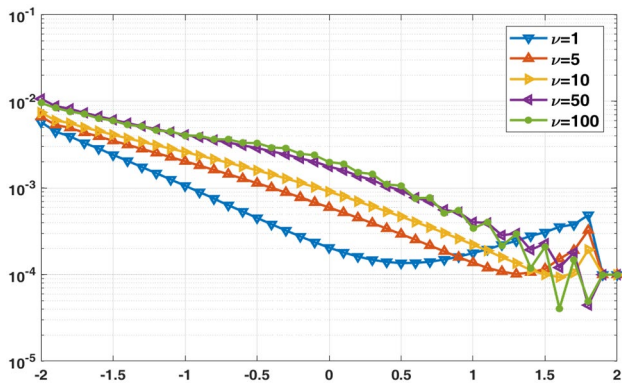
Fig. 6 Error obtained based on the values of v on domain Ω_2 for Example 1
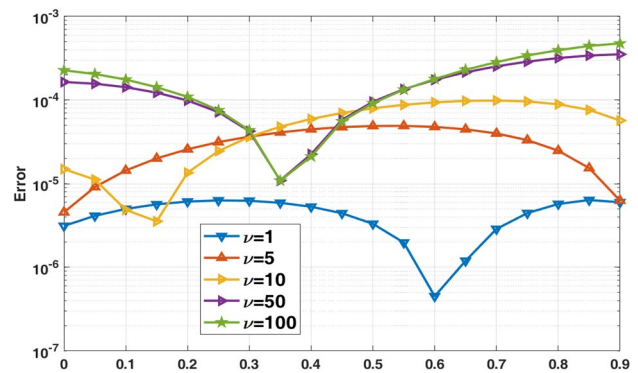
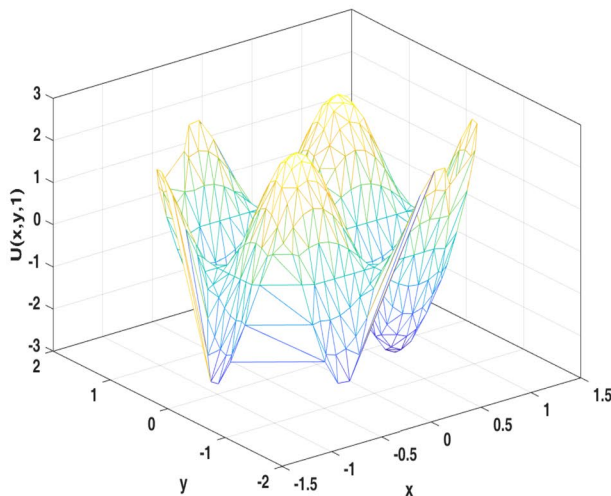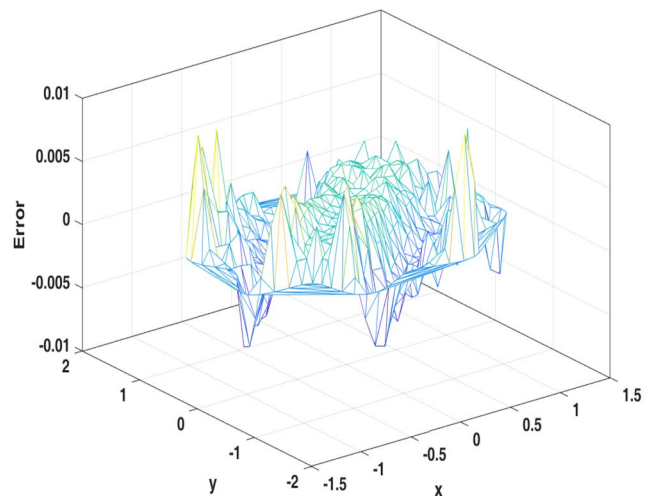**Fig. 8** Error obtained based on the values of v on domain Ω_3 for Example 1

Fig. 7 Graph of approximate and error with $v = 10$ on domain Ω_2 for Example 1
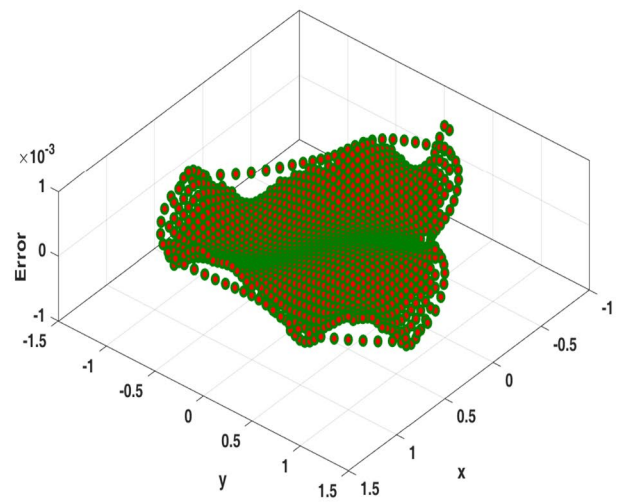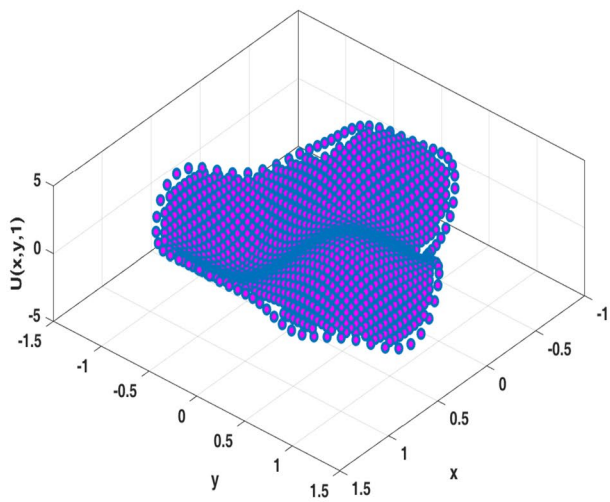
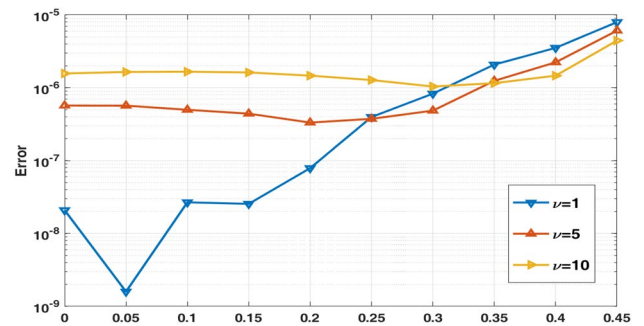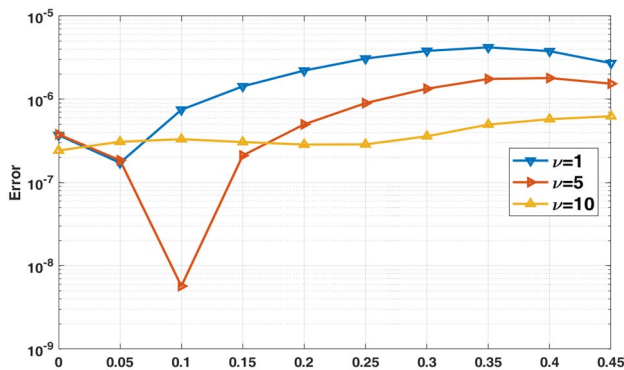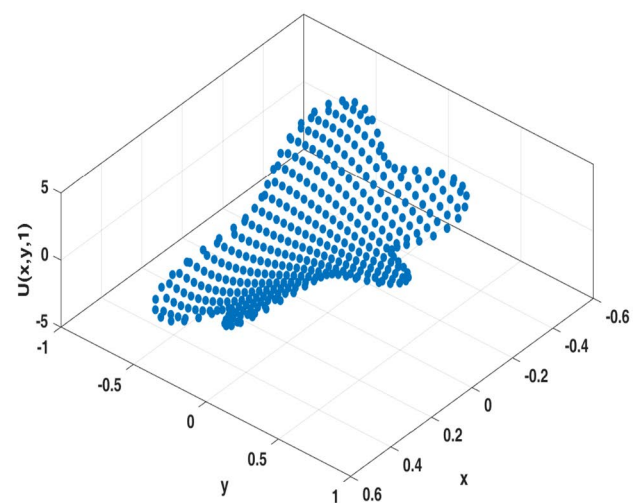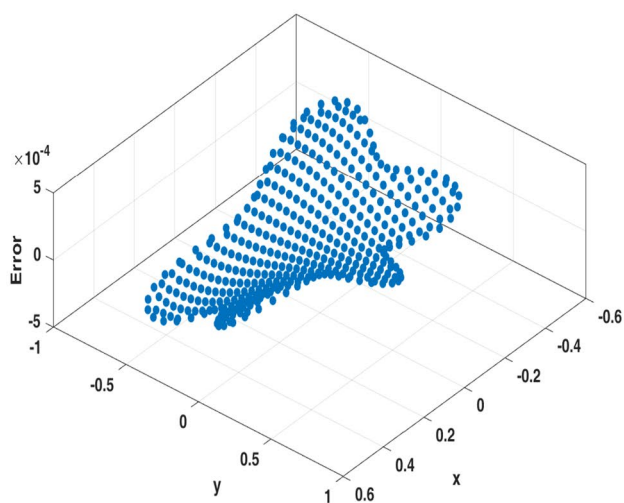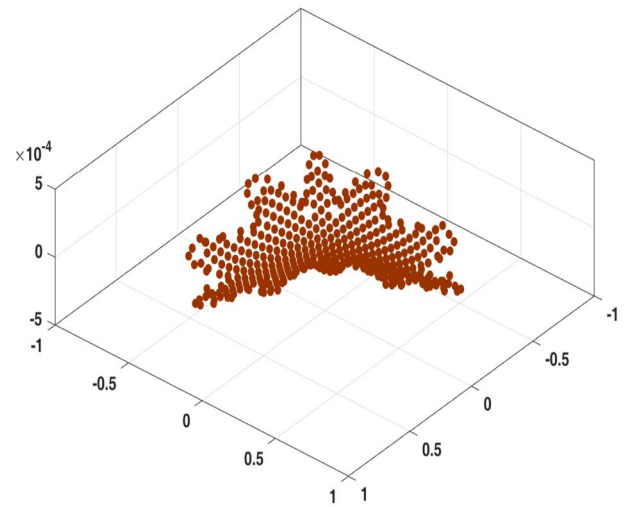**Fig. 9** Graph of approximate and error with $v = 10$ on domain Ω_3 for Example 1

Fig. 10 Error obtained based on the values of v on domain Ω_4 for Example 1

Fig. 12 Error obtained based on the values of v on domain Ω_4 for Example 1

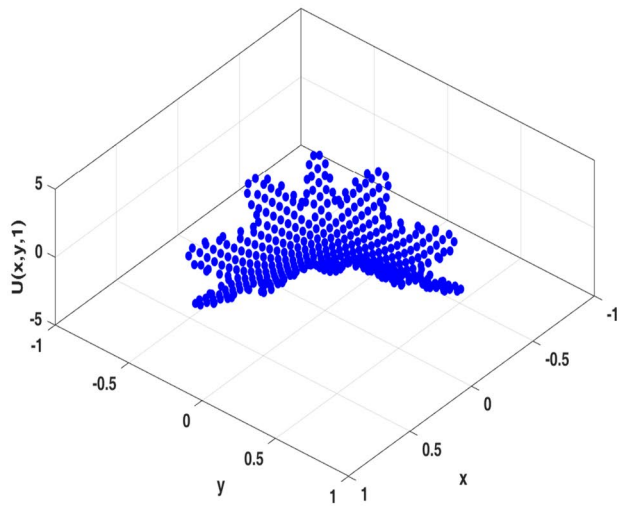**Fig. 11** Graph of approximate and error with $v = 10$ on domain Ω_4 for Example 1

Fig. 13 Graph of approximate and error with $\nu = 10$ on domain Ω_4 for Example 1
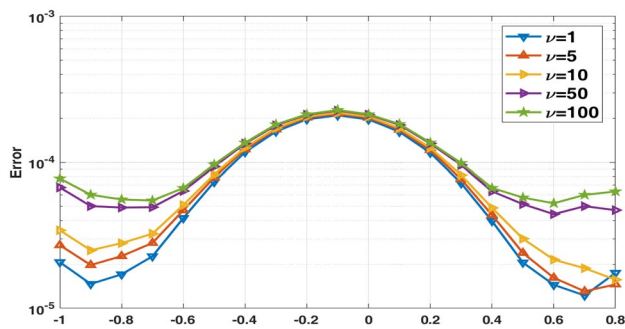

Fig. 14 Error obtained with $\sigma = 7/4$ for Example 2

5 Conclusion

In the current manuscript, the fractional distributed-order advection–diffusion equation has been investigated by a truly meshless method. In the developed technique, the time derivative has been approximated by a finite difference scheme. As well as, the spatial variable has been discretized by a meshless local procedure based on the upwind RBF-FD technique. The effect of the advection coefficient has been checked in the approximation results. Also, the used technique has been applied on some irregular domains. The stability and convergence of the proposed method are numerically studied.
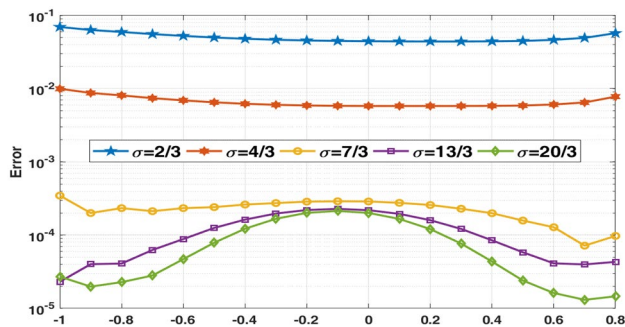

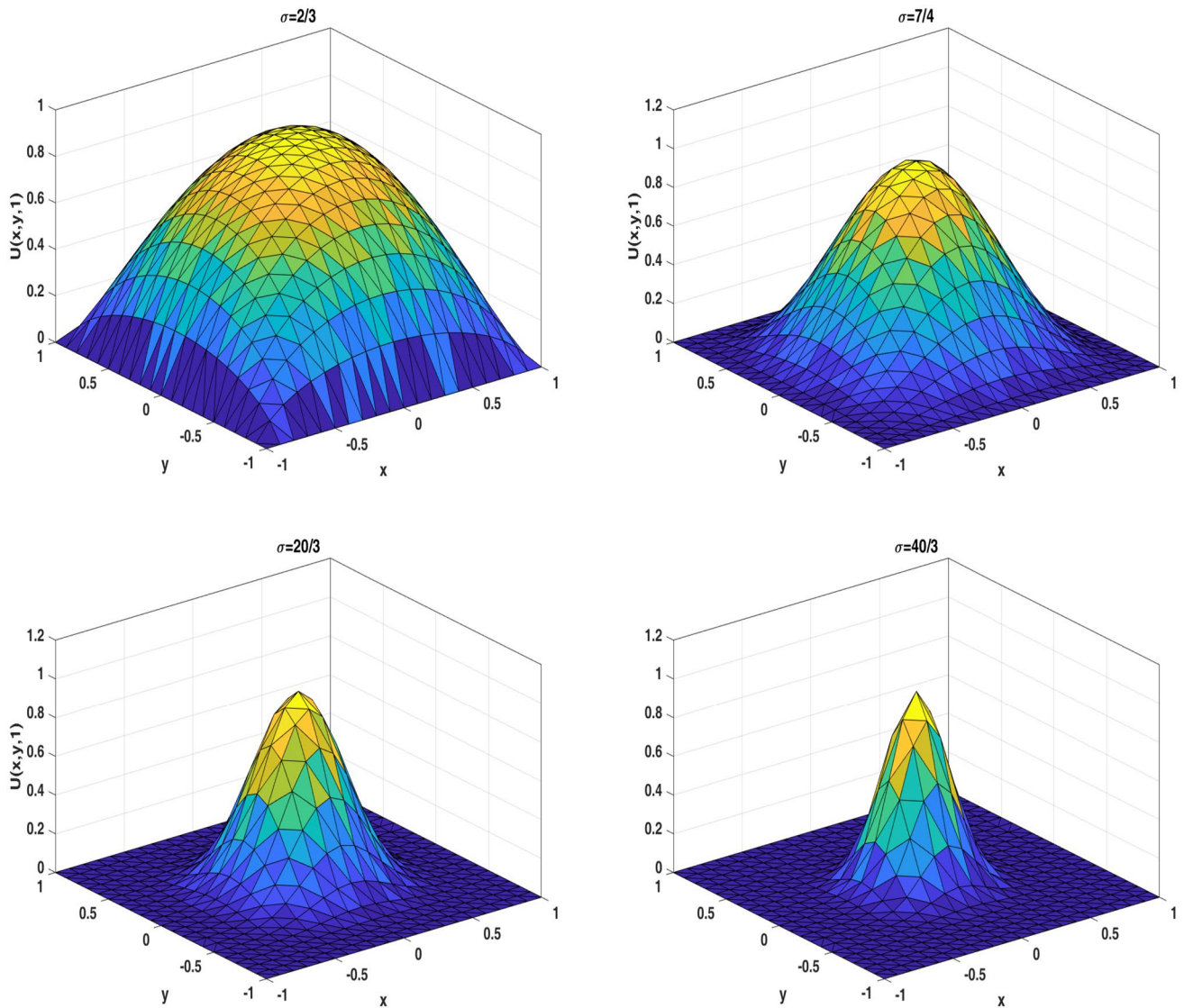**Fig. 15** Error obtained with $\nu = 50$ for Example 2

Fig. 16 Approximate solution with $\nu = 50$ for Example 2

Table 3 Errors achieved with $\tau = 10^{-5}$ for Example 2

N	$\sigma = \frac{4}{3}$		$\sigma = \frac{13}{3}$	
	$\nu = 10$	$\nu = 50$	$\nu = 10$	$\nu = 50$
20	2.0012×10^{-2}	6.2289×10^{-2}	2.2141×10^{-1}	8.8852×10^{-1}
40	8.6321×10^{-3}	2.0130×10^{-2}	7.3320×10^{-2}	2.3310×10^{-1}
60	3.0342×10^{-3}	8.8896×10^{-3}	2.1400×10^{-2}	6.5632×10^{-2}
80	9.7850×10^{-4}	4.1401×10^{-3}	8.7786×10^{-3}	1.0032×10^{-2}
120	4.0021×10^{-4}	1.0310×10^{-3}	3.0030×10^{-3}	8.9031×10^{-3}
150	1.0042×10^{-4}	8.9762×10^{-4}	1.1101×10^{-3}	4.0301×10^{-3}
200	8.0011×10^{-5}	4.0020×10^{-4}	8.8852×10^{-4}	1.0301×10^{-3}

References

1. Abbaszadeh M (2019) Error estimate of second-order finite difference scheme for solving the Riesz space distributed-order diffusion equation. Appl Math Lett 88:179–185
2. Abbaszadeh M, Dehghan M (2017) An improved meshless method for solving two-dimensional distributed order time-fractional diffusion-wave equation with error estimate. Numer Algorithms 75:173–211

3. Aliyu AI, Inc M, Yusuf A, Baleanu D (2018) A fractional model of vertical transmission and cure of vector-borne diseases pertaining to the Atangana–Baleanu fractional derivatives. Chaos Solitons Fractals 116:268–277

4. Atanackovic T, Pilipovic S, Zorica D (2009) Existence and calculation of the solution to the time distributed order diffusion equation. Phys Scr 2009(T136):014012

5. Atanackovic TM, Pilipovic S, Zorica D (2009) Time distributed-order diffusion–wave equation. i. Volterra-type equation. In: Proceedings of the Royal Society of London A: Mathematical, Physical and Engineering Sciences, The Royal Society, pp rspa–2008

6. Atangana A, Koca I (2016) Chaos in a simple nonlinear system with Atangana–Baleanu derivatives with fractional order. Chaos Solitons Fractals 89:447–454

7. Atangana A, Gomez-Aguilar JF (2018) Fractional derivatives with no-index law property: application to chaos and statistics. Chaos Solitons Fractals 114:516–535

8. Atkinson KE An introduction to numerical analysis, New York, p 528

9. Bhrawy AH, Zaky MA (2018) Numerical simulation of multi-dimensional distributed-order generalized Schrodinger equations. Nonlinear Dyn 89:1415–1432

10. Chechkin A, Gorenflo R, Sokolov I (2002) Retarding subdiffusion and accelerating superdiffusion governed by distributed-order fractional diffusion equations. Phys Rev E 66(4):046129

11. Chechkin AV, Gorenflo R, Sokolov IM, Gonchar VY (2003) Distributed order time fractional diffusion equation. Fract Calc Appl Anal 6(3):259–280

12. Dehghan M (2004) Weighted finite difference techniques for the one-dimensional advection–diffusion equation. Appl Math Comput 147(2):307–319

13. Dehghan M, Abbaszadeh M (2018) A Legendre spectral element method (SEM) based on the modified bases for solving neutral delay distributed-order fractional damped diffusion-wave equation. Math Methods Appl Sci 41:3476–3494

14. Dehghan M, Abbaszadeh M (2017) A finite element method for the numerical solution of Rayleigh–Stokes problem for a heated generalized second grade fluid with fractional derivatives. Eng Comput 33:587–605

15. Dehghan M, Abbaszadeh M (2019) Error estimate of finite element/finite difference technique for solution of two-dimensional weakly singular integro-partial differential equation with space and time fractional derivatives. J Comput Appl Math 356:314–328

16. Dehghan M, Manafian J, Saadatmandi A (2010) Solving nonlinear fractional partial differential equations using the homotopy analysis method. Numer Methods Partial Differ Equ 26:448–479

17. Ding H, Li CP (2019) A high-order algorithm for time-caputo-tempered partial differential equation with Riesz derivatives in two spatial dimensions. J Sci Comput 80:81–109

18. Ding H (2019) A high-order numerical algorithm for two-dimensional time-space tempered fractional diffusion-wave equation. Appl Numer Math 135:30–46

19. Ding H, Li CP (2018) High-order numerical approximation formulas for Riemann–Liouville (Riesz) tempered fractional derivatives: construction and application (II). Appl Math Lett 86:208–214

20. Ding H, Li CP (2017) High-order numerical algorithms for Riesz derivatives via constructing new generating functions. J Sci Comput 71(2):759–784

21. Driscoll TA, Fornberg B (2002) Interpolation in the limit of increasingly flat radial basis functions. Comput Math Appl 43(3–5):413–422

22. Eshaghi J, Kazem S, Adibi H (2018) The local discontinuous Galerkin method for 2D nonlinear time-fractional advection-diffusion equations. Eng Comput 1:4. https://doi.org/10.1007/s00366-018-0665-8

23. Flyer N, Lehto E, Blaise S, Wright GB, St-Cyr A (2012) A guide to RBF-generated finite differences for nonlinear transport: shallow water simulations on a sphere. J Comput Phys 231(11):4078–4095

24. Fornberg B, Lehto E (2011) Stabilization of RBF-generated finite difference methods for convective PDEs. J Comput Phys 230(6):2270–2285

25. Gao G-H, Sun Z-Z (2015) Two alternating direction implicit difference schemes with the extrapolation method for the two-dimensional distributed-order differential equations. Comput Math Appl 69(9):926–948

26. Javed A, Djijdeli K, Xing J (2014) Shape adaptive RBF-FD implicit scheme for incompressible viscous Navier–Stokes equations. Comput Fluids 89:38–52

27. Hafez RM, Zaky MA (2019) High-order continuous Galerkin methods for multi-dimensional advection-reaction-diffusion problems. Eng Comput. https://doi.org/10.1007/s00366-019-00797-y

28. Katsikadelis JT (2014) Numerical solution of distributed order fractional differential equations. J Comput Phys 259:11–22

29. Li C, Deng W, Zhao L (2019) Well-posedness and numerical algorithm for the tempered fractional differential equations. Discret Contin Dyn Syst B 24:1989

30. Luchko Y (2009) Boundary value problems for the generalized time-fractional diffusion equation of distributed order. Fract Calc Appl Anal 12(4):409–422

31. Hu X, Liu F, Turner I, Anh V (2016) An implicit numerical method of a new time distributed-order and two-sided space-fractional advection–dispersion equation. Numer Algorithms 72:393–407

32. Mashayekhi S, Razzaghi M (2016) Numerical solution of distributed order fractional differential equations by hybrid functions. J Comput Phys 315:169–181

33. Moghaddam BP, Machado JAT, Morgado ML (2019) Numerical approach for a class of distributed order time fractional partial differential equations. Appl Numer Math 136:152–162

34. Osman SA, Langlands TAM (2019) An implicit Keller Box numerical scheme for the solution of fractional subdiffusion equations. Appl Math Comput 348:609–626

35. Podlubny I, Skovranek T, Jara BMV, Petras I, Verbitsky V, Chen Y (2013) Matrix approach to discrete fractional calculus iii: non-equidistant grids, variable step length and distributed orders. Philos Trans R Soc A 371(1990):20120153

36. Qiao Y, Zhai S, Feng X (2017) RBF-FD method for the high dimensional time fractional convection–diffusion equation. Int Commun Heat Mass Transfer 89:230–240

37. Sandev T, Chechkin AV, Korabel N, Kantz H, Sokolov IM, Metzler R (2015) Distributed-order diffusion equations and multifractality: models and solutions. Phys Rev E 92(4):042117

38. Shankar V (2017) The overlapped radial basis function-finite difference (RBF-FD) method: a generalization of RBF-FD. J Comput Phys 342:211–228

39. Shu C, Ding H, Chen H, Wang T (2005) An upwind local RBF-DQ method for simulation of inviscid compressible flows. Comput Methods Appl Mech Eng 194(18–20):2001–2017

40. Sun Z-Z, Wu X (2006) A fully discrete difference scheme for a diffusion-wave system. Appl Numer Math 56(2):193–209

41. Wang X, Deng W Discontinuous Galerkin methods and their adaptivity for the tempered fractional (convection) diffusion equations. arXiv:1706.02826 (arXiv preprint)

42. Wendland H (2004) Scattered data approximation, vol 17. Cambridge University Press, Cambridge

43. Ye H, Liu F, Anh V (2015) Compact difference scheme for distributed-order time-fractional diffusion-wave equation on bounded domains. J Comput Phys 298:652–660

44. Yuttanana B, Razzaghi M (2019) Legendre wavelets approach for numerical solutions of distributed order fractional differential equations. Appl Math Model 70:350–364

45. Zaky MA (2018) An improved tau method for the multi-dimensional fractional Rayleigh–Stokes problem for a heated generalized second grade fluid. Comput Math Appl 75:2243–2258

46. Zaky MA, Machado JAT (2017) On the formulation and numerical simulation of distributed-order fractional optimal control problems. Commun Nonlinear Sci Numer Simul 52:177–189

47. Zaky MA, Doha EH, Machado JAT (2018) A spectral numerical method for solving distributed-order fractional initial value problems. J Comput Nonlinear Dyn 3(10):101007

48. Zaky MA (2018) A Legendre collocation method for distributed-order fractional optimal control problems. Nonlinear Dyn 91:2667–2681

49. Zaky MA (2019) Existence, uniqueness and numerical analysis of solutions of tempered fractional boundary value problems. Appl Numer Math. https://doi.org/10.1016/j.apnum.2019.05.008

50. Zaky MA (2019) Recovery of high order accuracy in Jacobi spectral collocation methods for fractional terminal value problems with non-smooth solutions. J Comput Appl Math 357:103–122

51. Zaky MA, Ameen IG (2019) A priori error estimates of a Jacobi spectral method for nonlinear systems of fractional boundary value problems and related Volterra–Fredholm integral equations with smooth solutions. Numer Algorithms. https://doi.org/10.1007/s11075-019-00743-5

52. Zayernouri M, Karniadakis GE (2014) Discontinuous spectral element methods for time-and space-fractional advection equations. SIAM J Sci Comput 36(4):B684–B707

53. Zhao X, Sun Z-Z, Karniadakis GE (2015) Second-order approximations for variable order fractional derivatives: algorithms and applications. J Comput Phys 293:184–200